

Nanoscale Reaction Vessels: Highly Ordered Nanocrystal Arrays inside Porous Anodic Alumina Nanowells

Hyeji Park¹, Tae-Hyeong Kim², Sang-Woo Kang³ and Soo-Hwan Jeong^{1,*}

¹ Department of Chemical Engineering, Kyungpook National University, Daegu 702-701, South Korea

² Department of Biomedical Engineering, Ulsan National Institute of Science and Technology (UNIST), Ulsan 689-798, South Korea

³ Division of Industrial Metrology, Korea Research Institute of Standards and Science (KRISS), Daejeon 305-340, South Korea

*E-mail: shjeong@knu.ac.kr

Received: 15 June 2015 / Accepted: 28 July 2015 / Published: 26 August 2015

Using an anodic alumina template as a nanoscale reaction vessel, the authors developed a simple and unique method to prepare highly ordered arrays of nanocrystals in isolated nanowells. The highly ordered arrays of nanoscale wells were fabricated by short anodization. After the nanoscale wells were filled with a precursor solution of NaCl by dewetting, the solvent of the precursor solution was evaporated, resulting in spontaneous formation of uniformly sized NaCl nanocrystals inside the nanoscale wells. The size of crystals could be easily adjusted by varying the concentration of the precursor solution and the size of nanoscale wells. This approach is simple and cost-effective, and it can fabricate nanocrystal arrays on substrates with high throughput. It can also be readily adapted to synthesize other types of high-density nanocrystal arrays on different substrates.

Keywords: Nanostructures, NaCl nanocrystals, Solution phase synthesis, Anodic alumina template.

1. INTRODUCTION

Functional structures consisting of nanocrystal arrays have recently been realized in the field of nanodevices such as optoelectronics, information storage, and sensing [1–9]. Although lithographic techniques offer good control over the nanocrystal size, shape, and spacing, these techniques involve expensive and time-consuming processes. One alternative and promising technique for preparing nanocrystal arrays might be the utilization of self-organized structures as initial building templates [10–12]. Among these techniques, approaches based on anodic aluminum oxide (AAO) templates have been successfully applied to form nanocrystal arrays. It is well known that an AAO template or mask

offers considerable simplicity and convenience in fabrication because it can be used to form structures with high-density, well-ordered sub-100-nm pores and offers the ability to easily control the pore dimensions. Therefore, the AAO-template-assisted approach has been considered as a complement to conventional lithographic techniques for fabricating simple sub-100-nm nanodot arrays.

Currently, two strategies have been proposed for synthesizing nanodot arrays using AAO. One method is based on direct deposition, such as electroplating, of nanodot materials at the bottom of AAO pores [13-16]; however, the choice of materials for electrochemical deposition is very limited. The other method of preparing nanocrystal arrays utilizes AAO membranes as an evaporation mask, with through-hole AAO membranes prepared from a bulk Al sheet and then placed on a substrate [8, 17-19]. For example, Masuda et al. used AAO membranes as an evaporation mask to prepare metal nanodot arrays on a silicon wafer [17,18].

However, the reproducibility and precise positioning of the technique are inadequate because AAO membrane masks lack sufficient adhesion to the substrates. Moreover, it is very difficult to handle this type of mask because the membrane must be very thin for successful electron-beam evaporation, and its use is limited to a small area (approximately several mm² ~ one cm²) owing to the membrane's tendency to crack during detachment from the Al layer. It should be noted that the diameters of nanocrystals produced using both methods are almost the same as that of pores in an AAO template. To reduce the size of metal nanodot formed in this method, partial oxidation of surface and subsequent etching was carried out [8].

On the other hand, nanocrystal growth inside the nanowell arrays, which was prepared through imprint lithography [20] or photolithography has been studied [21,22]. In these cases, insertion of nanowell substrate into a precursor solution and subsequent discontinuous dewetting resulted in the formation of smaller diameter nanodot inside the nanowell arrays than that of nanowell size. For example, Barton et al. [20] prepared nanowells with nanoscale volumes by laser-assisted imprint lithography and used them as nanoscale reaction vessels for the fabrication of nanodot arrays. Recently, the same group showed arsenic trioxide nanodot arrays inside the nanowell arrays which were produced by relatively complex lithographic technique [21].

Inspired by this dewetting method, we herein demonstrate that highly ordered nanowell arrays based on an AAO template with narrow size distribution, which can be formed by relatively short anodization, can serve as parallel reaction vessels for high-yield formation of highly ordered and isolated nanocrystals with dimensions that are completely different from those of the nanowell template. Specifically, we show that the evaporation of inorganic salt of a NaCl solution inside the pores forms a hexagonal array of isolated nanocrystals on the AAO template. The results show that the use of nonlithographic self-organized high-density nanowell arrays in an AAO template with evaporation-induced formation of nanodots can potentially be applied to the fabrication of high-density isolated nanodot arrays, which may be adapted into a general method of nanocrystal formation.

2. EXPERIMENTAL

The process used to create nanocrystals in the nanowell arrays of the AAO template is shown schematically in Figure 1. Our strategy begins with the preparation of highly ordered pore arrays of the

AAO template with low aspect ratio. Two-step anodization [23] was chosen for this purpose. In brief, a cleaned and electropolished Al sheet of high purity (99.999%, $1 \times 2 \text{ cm}^2$) was first anodized at 40 V in a 0.3 M oxalic acid solution at 15 °C for 12 h. After chemically etching the AAO film in a mixed solution of phosphoric acid and chromic acid, anodization was performed again under the same conditions for 50 s, which resulted in the formation of highly ordered nanowell arrays in the AAO template with a pore depth of 50 nm. To prepare nanoscale reactor vessels with the appropriate volume, the pore diameters of the AAO templates were adjusted to 50 or 80 nm by widening the pores in a 0.5 wt % phosphoric acid solution. Using the discontinuous dewetting method, the nanowell arrays were filled with 0.01 or 1 M NaCl aqueous solutions at 50 °C. The withdrawal speed was 0.8 cm/min. The solvent was then evaporated at 60 °C in an oven.

The morphology of the nanowell arrays and synthesized NaCl nanocrystals were observed with a field-emission scanning electron microscope (FE-SEM; S-4200, Hitachi, Japan). Further analysis of the formed nanocrystal arrays was performed with an X-ray diffractometer (XRD; D/MAX-2500, Rigaku, Japan) and a transmission electron microscope (TEM; JEM-2200FS, JEOL, Japan) equipped with an energy-dispersive spectrometer.

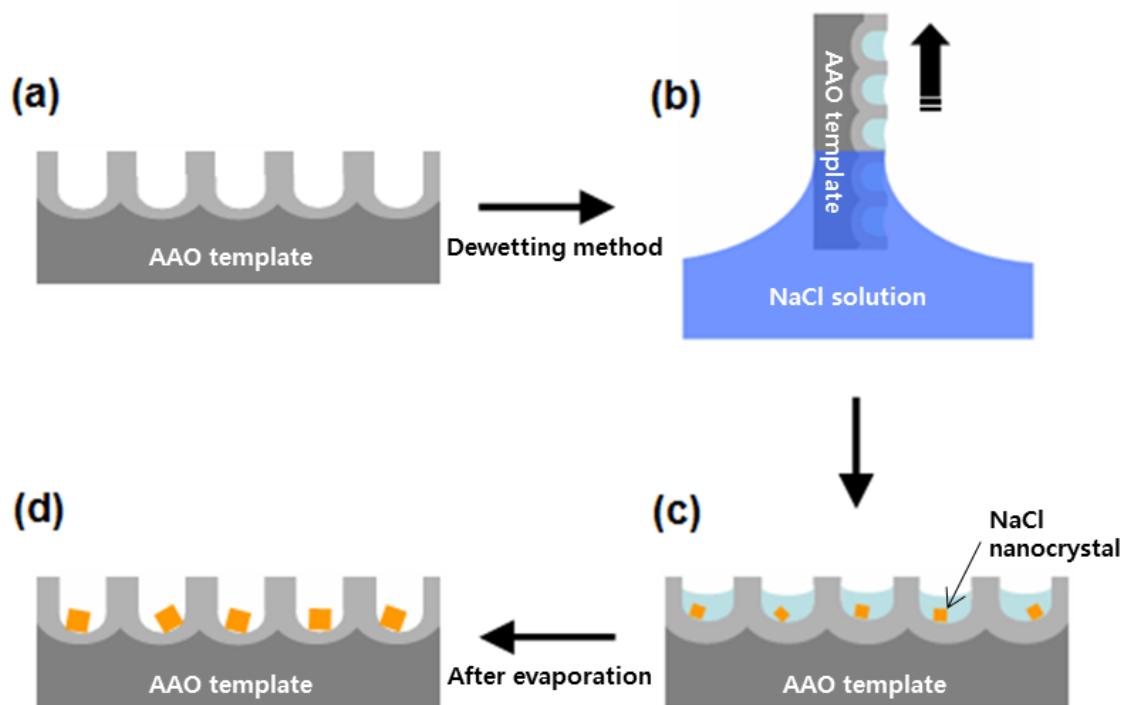


Figure 1. Schematic for the preparation NaCl nanocrystal in the nanowell arrays of AAO template.

3. RESULTS AND DISCUSSION

The SEM images in Figure 2 clearly show that the nanowells in the AAO template were formed periodic and hexagonal close-packed arrays.

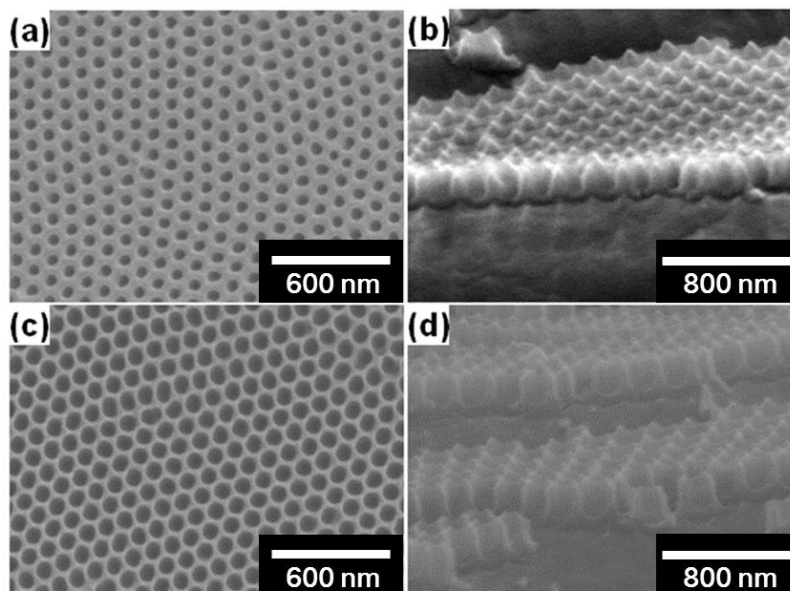


Figure 2. SEM image of the array of nanowells in AAO template after pore-widening for (a, b) 20 min, (c, d) 35 min.

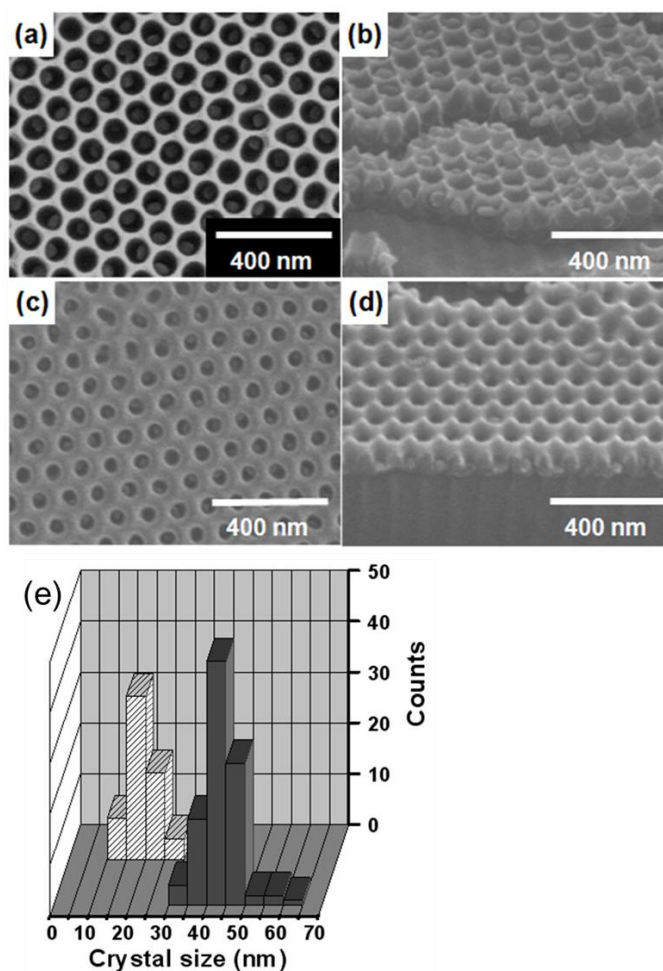


Figure 3. SEM images and nanocrystal size distribution of NaCl crystals inside the nanowell arrays: individual nanocrystals grown within (a, b) 80 nm wells from a 1 M NaCl solution and (c, d) 50 nm wells from a 0.01 M NaCl solution, (e) crystal size distributions for both cases.

The pore diameters were adjusted to 50 and 80 nm by widening process and density of pores was 1.0×10^{10} pores/cm² for both cases. The estimated volume of each pore was around 0.16 and 0.55 zL (one zeptoliter equals 1×10^{-21} L), respectively. The pitch (center-to-center distance of pores) of our nanowell arrays is 100 nm. This value is much smaller than those of lithography based nanowell arrays for crystal growth. For example, Odom and co-workers [21] photolithographically fabricated 2- μ m pitch nanowell arrays for growing nanocrystals. In order to increase the nanowell density, they also made 400-nm pitch nanowell arrays via soft interference lithography method. It is worth mentioning that our pore density is 16 times higher than that of 400-nm pitch nanowell arrays based on interference lithography.

Figure 3 shows SEM images of NaCl crystals inside the nanowell arrays after dewetting and evaporation. Most nanowells could eventually be filled with uniformly sized crystals, resulting in an overall high yield. By counting the number of nanowells occupied with the crystals in several SEM images, the average filling rates were estimated. The percentage of the occupied pores in Figure 3 was about 90%. We demonstrated convincingly how lower concentrations of precursors and smaller size of nanowells resulted in smaller nanoparticles by crystallizing NaCl. The concentration of the precursor solution was lowered from 1 to 0.01 M (Figures 3a and c) and the nanowell volume was simultaneously reduced from 0.55 to 0.16 zL. The 0.55-zL nanowells that were filled with a 1 M salt solution (Figure 3a and b) resulted in bigger crystals than those formed from the 0.01 M solution with a 0.16 zL nanowells (Figure 3c and d). The average crystal sizes for both cases were 43.2 (Figure 3a and b) and 18.4 nm (Figure 3c and d), respectively (Figure 3e). Unlike the previous reports regarding AAO template as an evaporation mask [8,20], size of nanocrystals inside the nanowells (zL) was smaller than pore sizes of nanowells. In addition, crystal size inside the nanowell could be easily controlled by varying the concentration of precursor solution.

Assuming that the prepared crystals had a cubic shape, a simple calculation for the comparison of crystal size prepared using AAO templates with nanowells of both sizes was carried out. From this estimation, the side length of the nanocrystals formed in the smaller nanowells must be one seventh of the length of those formed in the larger nanowells. However, the observed difference in the crystal sizes was only a factor of 2.4. Although the reason remains unclear at this time, we believe that this discrepancy might have partially resulted from the increased wettability of the NaCl solution on the AAO template with smaller pores after dewetting. Ran et al. demonstrated that the wettability of AAO was dramatically changed from hydrophilicity to hydrophobicity by increasing the hole diameter, and this phenomena was attributed to the gradual transition between the Wenzel and Cassie states [25]. Several important characteristics of this method should be noted. First, the sizes of the nanowells can be easily controlled by simply adjusting the parameter of pore-widening time after two-step anodization. Although we showed nanowells with the same depth, the dimensions of the nanowells could be easily controlled by varying the anodizing time and applied voltages during the anodization process. Since this method does not require lithography, it is simple and inexpensive. These nanoscale reaction wells based on the AAO template are ideal reaction vessels for the growth of nanocrystals. Because of their small volumes, uniform sizes, highly ordered arrays, high densities, and self-organized structures, the confined evaporation of precursor materials should enable the growth of

uniform and high-density nanocrystals in a highly ordered manner. These properties are very important to the fundamental characterization and potential applications of nanocrystal-based devices.

Figure 4(a) shows a TEM image of a NaCl crystal and its corresponding EDS pattern. The size of the crystal matches well with that shown in the SEM image in Figure 3(a). The EDS pattern confirms that the grown crystals consisted of sodium and chloride in an atomic ratio of 1:1, suggesting that the formed NaCl compound had an ionic bond. The XRD pattern in Figure 4(b) indicates that the formed nanoparticles had a crystalline nature and the NaCl nanocrystals grew in the (200) and (220) directions. The strong peak at about 45° represents reflection from the (200) plane of the Al substrate.

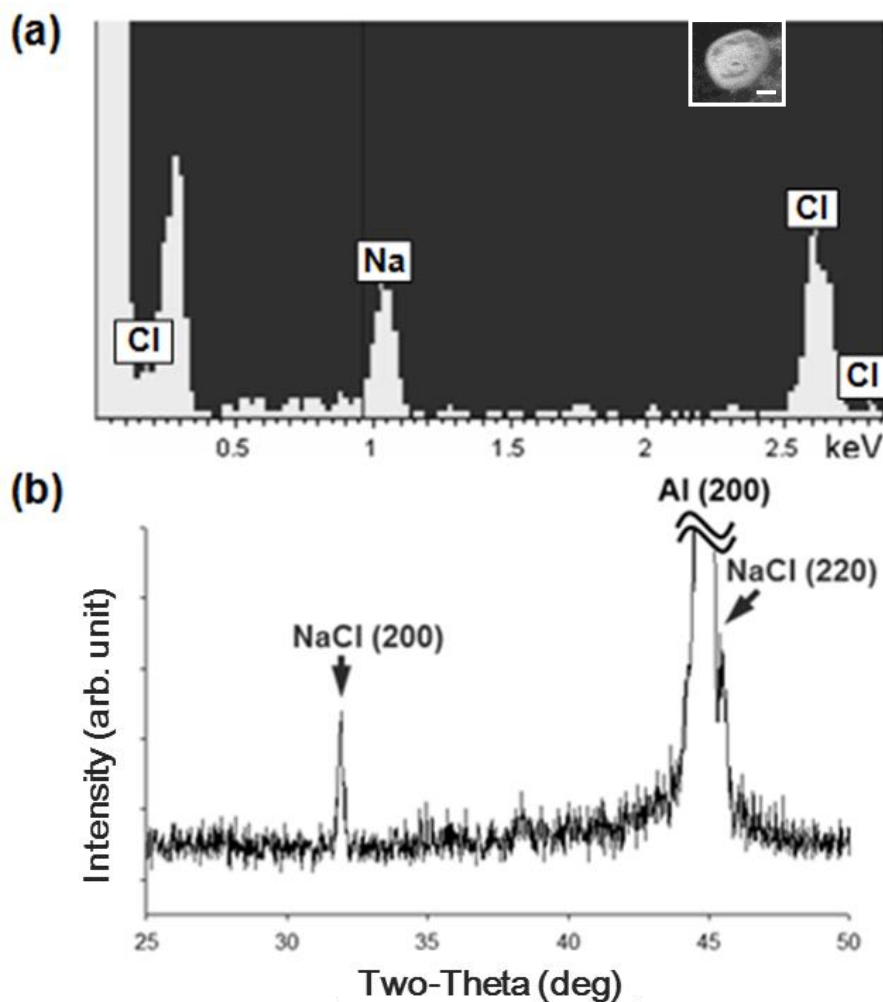


Figure 4. (a) TEM image of a NaCl crystal (scale bar is 20 nm) and its corresponding EDS pattern. (b) XRD pattern of NaCl nanocrystals that grew in the (200) and (220) directions.

4. CONCLUSIONS

We have developed a novel method for the growth of highly ordered nanocrystal arrays by using the self-organized nanowell structures as nanoscale reaction vessels. The size of the nanocrystals was easily adjusted by varying the concentration of the precursor solution and the volume of nanowells. This method can be a useful route for simple fabrication of high-density isolated

nanocrystals over a large area. Although we only showed the formation of NaCl crystals inside the nanoscale well arrays in the AAO template, it is expected that the proposed process can be easily applied to synthesize other kinds of nanocrystal arrays.

References

1. F. A. Reboredo, E. Schwegler and G. Galli, *J. Am. Chem. Soc.*, 125 (2003) 15243
2. X. Li, Y. Wu, D. Steel, D. Gammon, T. H. Stievater, D. S. Katzer, D. Park, C. Piermarocchi and L. S. Sham, *Science*, 301 (2003) 809
3. T. C. Harman, P. J. Taylor, M. P. Walsh and B. E. LaForge, *Science*, 297 (2002) 2229
4. V. I. Klimov, A. A. Mikhailovsky, Su Xu, A. Malko, J. A. Hollingsworth, C. A. Leatherdale, H.-J. Eisler and M. G. Bawendi, *Science*, 290 (2000) 314
5. S. Tiwari, F. Rana, H. Hanafi, A. Hartstein, E. F. Crabbe and C. Kevin, *Appl. Phys. Lett.*, 68 (1996) 1377
6. Z. Gai, J. Y. Howe, J. D. Guo, D. A. Blom, E. W. Plummer and J. Shen, *Appl. Phys. Lett.*, 86 (2005) 023107
7. J.-H. Han, L. Sudheendra, H.-J. Kim, J. S. Gee, B. D. Hammock and I. M. Kennedy, *ACS Nano*, 6 (2012) 8570
8. C. Zhao, Y. Zhu, Y. Su, Z. Guan, A. Chen, X. Ji, X. Gui, R. Xiang and Z. Tang, *Adv. Optical Mater.*, 3 (2015) 248
9. A. Sangar, A. Merlen, P. Torchio, S. Vedraïne, F. Flory, L. Escoubas, L. Patrone, G. Delafosse, V. Chevallier, E. Moyen and M. Hanbucken, *Sol. Energ. Mat. Sol. C.*, 117 (2013) 657
10. D. Routkevitch, A. A. Tager, J. Haruyama, D. Almawlawi, M. Moskovits and J. M. Xu, *IEEE Trans. Electron Devices*, 43 (1996) 1646
11. H. Deckman and J. H. Dunsmuir, *Appl. Phys. Lett.*, 41 (1982) 377
12. K. Douglas, G. Devaud and N. Clark, *Science*, 257 (1992) 642
13. H. Masuda, H. Tanaka and N. Baba, *Bull. Chem. Soc. Jpn.*, 66 (1993) 305
14. S. Shingubara, O. Okino, Y. Sayama, H. Sakaue and T. Takahagi, *Jpn. J. Appl. Phys.*, 36 (1997) 7791
15. J. L. Gong, D. Z. Zhu and H. H. Xia, *Nanotechnology*, 18 (2007) 015303
16. X. Yang, J. Hou, Y. Liu, M. Cui and W. Lu, *Nanoscale Res. Lett.*, 8 (2013) 328
17. H. Masuda and M. Satoh, *Jpn. J. Appl. Phys.*, 35 (1996) L126
18. H. Masuda, K. Yasui and K. Nishio, *Adv. Mater.*, 12 (2000) 1031
19. U. Malinovskis, R. Poplausks, I. Apsite, R. Meija, J. Prikulis, F. Lombardi and D. Erts, *J. Phys. Chem. C*, 118 (2014) 8685
20. J. E. Barton and T. W. Odom, *Nano Lett.*, 4 (2004) 1525
21. E.-A. You, R. W. Ahn, M. H. Lee, M. R. Raja, T. V. O Halloran and T. W. Odom, *J. Am. Chem. Soc.*, 131 (2009) 10863
22. J. W. Krumpfer and T. J. McCarthy, *J. Am. Chem. Soc.*, 133 (2011) 5764
23. H. Masuda and K. Fukuda, *Science*, 268 (1995) 1466
24. T. L. Wade and J.-E. Wegrowe, *Eur. Phys. J. Appl. Phys.*, 8 (2005) 3
25. C. Ran, G. Ding, W. Liu, Y. Deng and W. Hou, *Langmuir*, 24 (2008) 9952